Bioorganic Chemistry 76 (2018) 314–325

Contents lists available at ScienceDirect

Bioorganic Chemistry

journal homepage: www.elsevier.com/locate/bioorg

Novel 1,2,4-triazole derivatives as potential anticancer agents: Design, synthesis, molecular docking and mechanistic studies

Hany A.M. El-Sherief [a,c], Bahaa G.M. Youssif [b,c,*], Syed Nasir Abbas Bukhari [c], Mohamed Abdel-Aziz [d,*], Hamdy M. Abdel-Rahman [a,e]

[a] Department of Pharmaceutical Chemistry, Faculty of Pharmacy, Nahda University, Beni-suef, Egypt
[b] Department of Pharmaceutical Organic Chemistry, Faculty of Pharmacy, Assiut University, Assiut 71526, Egypt
[c] Department of Pharmaceutical Chemistry, College of Pharmacy, Aljouf University, Aljouf, Sakaka 2014, Saudi Arabia
[d] Department of Medicinal Chemistry, Faculty of Pharmacy, Minia University, 61519 Minia, Egypt
[e] Department of Medicinal Chemistry, Faculty of Pharmacy, Assiut University, 71526 Assiut, Egypt

ARTICLE INFO

Article history:
Received 1 October 2017
Revised 31 October 2017
Accepted 3 December 2017
Available online 5 December 2017

Keywords:
1,2,4-Triazole
Antiproliferative
EGFR
BRAF
Tubulin and molecular docking

ABSTRACT

A series of novel compounds carrying 1,2,4-triazole scaffold was synthesized and evaluated for their anticancer activity against a panel of cancer cell lines using MTT assay. Compounds **8a, 8b, 8c, 8d, 10b, 10e,** and **10 g** showed remarkable antiproliferative activity against the tested cell lines. Compounds **8a, 8b, 8c, 8d, 10b, 10e,** and **10 g** with the least IC_{50} values in MTT assay were tested against three known anticancer targets including EGFR, BRAF and Tubulin. The results revealed that compounds **8c** and **8d** showed almost same BRAF inhibitory activity and were discovered to be potent inhibitors of cancer cell proliferation and were also observed to be strong Tubulin inhibitors. Moreover, **8c** also showed the best EGFR inhibition with IC_{50} = 3.6 μM. Finally molecular modeling studies were performed to explore the binding mode of the most active compounds to the target enzymes.

1. Introduction

Cancer is one of the powerful life threatening diseases [1]. Literature showed that more than 90% of cancer patients die due to chronic tumor metastases [2]. Additionally, targeted cancer therapies are drugs that block the growth and spread of cancer by interfering with specific molecules that are involved in the growth, progression, and spread of cancer. Target variety of cancer therapy as hormone therapy, angiogenesis inhibitors and apoptosis inducers provided researchers with different options to concer with each of them [3,4]. Many of vital cellular processes like cell proliferation, cell shape regularity and mitotic spindle formation exhibited the significant role of microtubule system in cell life [5]. The importance of microtubule system in mammalian cell has made them an attractive target for the development of drugs such as anticancer agents [6]. Microtubule-targeting agents can be divided into two main groups depending on their mechanisms of actions microtubule-stabilizing agents (MSA) and microtubule destabilizing agents (MDA) [7]. MSAs prefer to bind to the polymerized tubulins and stabilize microtubules, while MDAs prefer to bind to the tubulin dimers and destabilize microtubules [8]. There are three well-characterized drug binding sites on tubulin: taxol, vinca, and colchicine sites [9]. Drugs that bind to the first two sites, such as paclitaxel (taxol) and vinblastine, have been successfully used in clinics as chemotherapeutics to treat various tumor types; however, their use is limited by multiple drug resistance (MDR). On the other hand, several colchicine site binders have been shown to inhibit MDR tumors, instilling renewed interest in the search for novel antimitotic agents that bind to the colchicine binding site on tubulin [10]. Combretastatin A-4 (CA-4) and its more soluble analog combretastatin A-4 phosphate (CA-4P) are tubulin polymerization inhibitors; CA-4 has the ability to disrupt microtubule dynamics and hence mitotic spindle by binding to colchicine binding site in a tubulin dimer. It also causes occlusion of tumor vasculature resulting in hypoxia-driven necrosis focused on the core of the tumor [11,12]. During the last few decades, a considerable attention has been devoted to 1,2,4-triazole derivatives due to their wide spectrum of biological activities such as anticonvulsant [13], anticancer, antidepressant [14], antibacterial [15], antifungal [16], anti-inflammatory, analgesic [17] and antiviral activities [18]. The discovery of CA-4 has led to a diverse library of antitumor agents, due to simple structure and great anticancer potency [19–21]. The SAR studies indicated that the presence of a

* Corresponding authors at: Department of Pharmaceutical Organic Chemistry, Faculty of Pharmacy, Assiut University, Assiut 71526, Egypt (B.G.M. Youssif).
E-mail addresses: bgyoussif@ju.edu.sa (B.G.M. Youssif), Abulnil@hotmail.com (M. Abdel-Aziz).

https://doi.org/10.1016/j.bioorg.2017.12.013
0045-2068/

3,4,5-trimethoxyphenyl ring-A and *cis*-double bond is essential for potent anticancer activity [22]. As a result, a significant number of the conformationally restricted analogues obtained by incorporating the *cis*-olefin bridge into a heterocyclic ring system have been investigated [23–26]. Among them 1,2,4-triazole-containing analogues [27] have been reported to possess potent antiproliferative activities comparable to CA-4. Compound **I** inhibited bovine brain tubulin polymerization *in vitro* by 80% and depolymerized microtubules in cultured A431 cells within 20 min. (Fig. 1). Compound **I** also demonstrated antiproliferative activity against several tumor cell lines and induced G2/M arrest of A431 human cancer cells [10]. Compound **II** exhibited high inhibitory activity against CEM and hela cells with IC_{50} of 0.21 nm and 3.2 nm, respectively [28].

Additionally aralkyl isothiocyanates have been established to exhibit antiproliferative activities against fungi and bacteria, particularly gram-positive bacteria [29–31]. Recently, they have been implicated in mediating antitumor activities. These compounds have inhibitory effects on the growth of several types of cultured cancer cells, including leukemia [32,33], prostate cancer [34], breast cancer [35], lung cancer [36,37], cervical cancer [38], and colorectal cancer [39]. Studies have implicated numerous pathways for the anticancer activity of isothiocyanates including; induction of apoptosis [40], induction of cellular oxidative stress [41] cell cycle arrest in different phases [42,43], inhibition of angiogenesis [44], inhibition of histone deacetylation [45] and inhibition of cell cycle progression [46].

Based on the aforementioned facts, the objectives of this study aimed to design and synthesis of some novel 1,2,4-triazole derivatives, where the presence of 1,2,4-triazole ring would augment the bioavailability and chemical stability. The steric and electronic effects of different electron donating alkoxy groups on the benzene moiety of ring A and B were chosen to improve the cytotoxicity and physicochemical properties of these compounds. Additionally a novel hybrid of 1,2,4-triazole/isothiocyanates were prepared by gathering the two bioactive entities 1,2,4-triazole and isothiocyanates in one compact structure for the purpose of synergism (see Fig. 2), the prepared compounds were identified using different spectroscopic techniques including: IR, ^{1}H NMR, ^{13}C NMR as well as high resolution mass HRMS. The designed compounds were assessed for their antitumor activity through *in vitro* cytotoxicity study on selected human cancer cell lines. Moreover, the mechanistic studies were also evaluated on $BRAF^{V600E}$, EGFR TK kinases and tubulin polymerization.

2. Results and discussion

2.1. Chemistry

Compounds **3a-b** were prepared in 90–95% yield by fusion of the respective pyridine carboxylic acids **1a** or **1b** and aminoguanidine sulfate at 210 °C for 2 h [47]. Arylamidoguanidines **6a-e** were prepared by reaction of benzohydrazide **5a-e** with methyl isothiourea (Scheme 1) [48–50]. Heating at reflux of arylamidoguanidines **6a-e** in water underwent quantitative cyclocondensation with elimination of water affording 3(5)-amino-5(3)-aryl-1,2,4-triazoles **7a-e** [51,52]. Stirring at room temperature compounds **3a-b** or **7a-e** with different acid chlorides or alky isothiocyanates afforded the target compounds **8a-f**, **9a-f**, **10a-g** and **11a-f**, respectively (see Scheme 2). The structure of the newly synthesized compounds **8a-f, 9a-f**, **10a-g** and **11a-f** was confirmed on the basis of IR, ^{1}H NMR, ^{13}C NMR spectroscopic data as well as high resolution mass.

IR spectra of compounds **8a-d** showed a significant stretching forked peak at 3110–3150 cm^{-1} due to NH_2 group. While in compounds **8e-f** a significant sharp peaks appear in the region of 3390–3400 cm^{-1} due to presence of NH gp of triazole. On the other hand, a characteristic intense peak at 3230–3250 cm^{-1} indicating the presence of amidic NH. Moreover, a sharp intense peak at 1690–1695 cm^{-1}, corresponds to carbonyl group of 2ry amide CO-N in compounds **8a-d**, while in compounds **8e-f** appears at the region of 1635–1640 cm^{-1}.

The ^{1}H NMR spectra of compounds **8a-d** exhibited a singlet signal at δ 7.15–7.90 ppm (2H) corresponding to NH_2. A singlet signal at δ 10.29–10.42 ppm (1H) corresponding to NH amide, while NH-triazole appears at 10.58 ppm. Moreover, the ^{1}H NMR of the aromatic protons in compounds **8a-f** exhibited two doublets at δ 7.03–7.14 ppm (2H) and 7.92–8.29 ppm (2H) corresponding to Para disubstitution of benzoyl ring. In addition, ^{1}H NMR of compound **8e** showed a characteristic signal at δ 3.84 ppm (3H, s) corresponding to *p*-OCH_3, while in compound **8b** the ^{1}H NMR spectrum showed two signals at 3.72 and 3.85 ppm of 3,4,5-triOCH_3. ^{13}C NMR spectra of compounds **10a-f** exhibited significant signals at δ 56, 60 ppm related to OCH_3 gp, 162–163 ppm corresponding to C=O gp of amide either in compounds **8a-d** or **8e-f.**

IR spectra of compounds **9a-c** showed forked peak at 3115–3130 cm^{-1} due to NH_2 group, while compounds **9d-e** exhibited sharp peaks at 3395–3415 cm^{-1} due to NH gp of triazole. On the other hand, characteristic intense peak appears at 3235–3255 cm^{-1} indicating for NH amide of triazole. In addition, another sharp intense peak at 1685–1695 cm^{-1}, characteristic for CO-N group in compounds **9a-c**, while in compounds **9d-e** it appears at the region of 1645–1650 cm^{-1}.

The ^{1}H NMR spectra of compounds **9a-c** showed a singlet signal at δ 7.81–8.09 ppm (2H) corresponding to NH_2 group and a singlet signals at δ 10.31–10.55 ppm (2H) corresponding to CO-NH amide and NH-triazole. In addition compound **9** showed a singlet (3H) at δ 3.83 ppm corresponding to OCH_3, two singlets at 3.72 and 3.87 ppm (9H) corresponding to 3,4,5-triOCH_3 and two singlets at 3.79 and 3.89 ppm (6H) corresponding to 3,4-diOCH_3**.** ^{13}C NMR spectra of compound **9a-e** showed significant peaks at δ 55, 56, 60 ppm related to OCH_3 group, 165–167 ppm related to C=O group of amide.

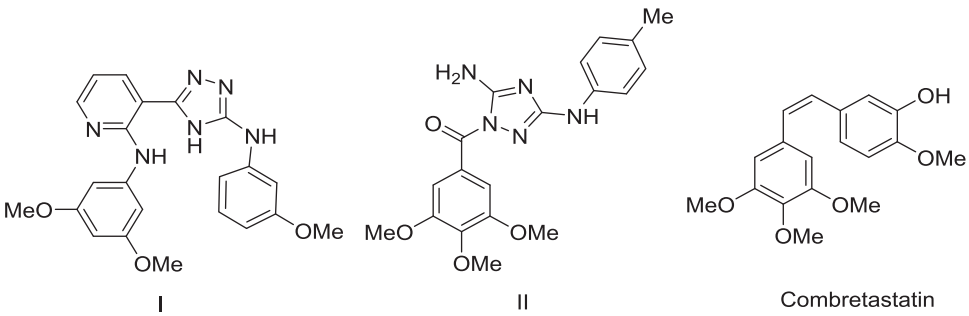

Fig. 1. Structures of compounds **I, II** and combretastatin.

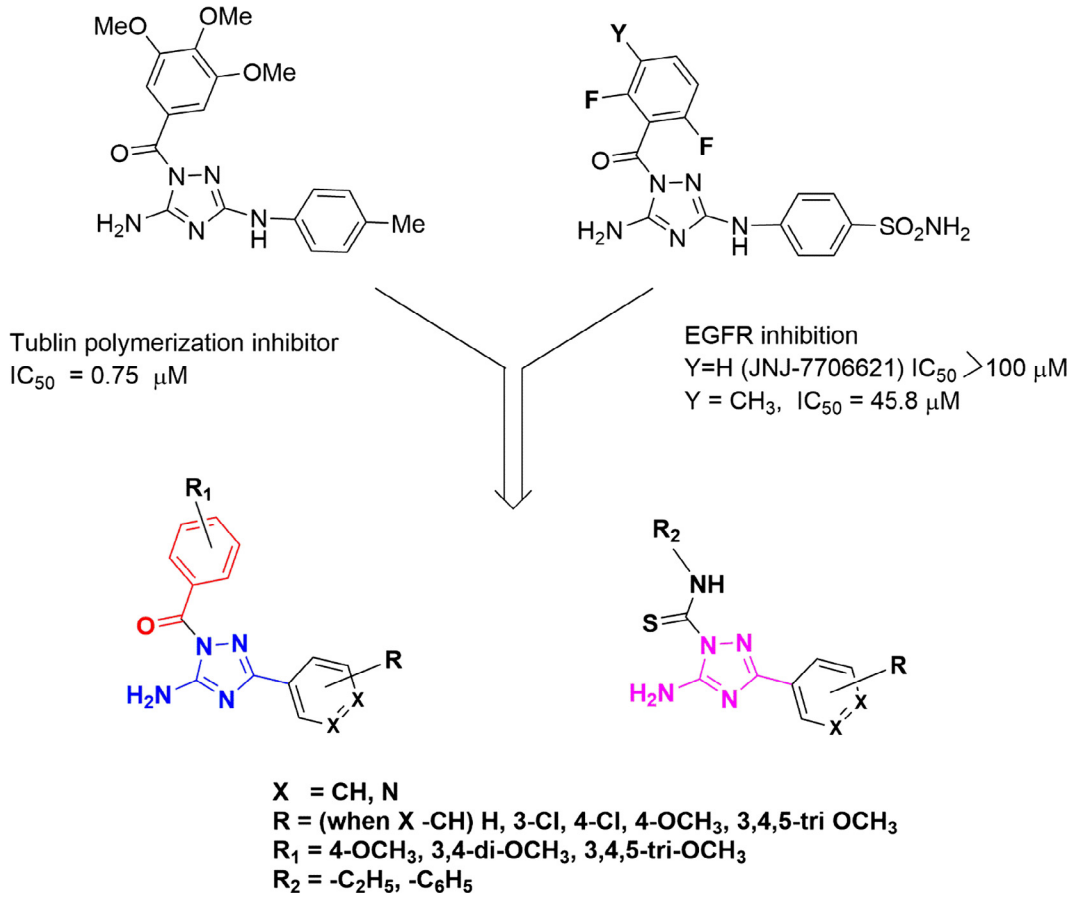

Fig. 2. The design rationale for the final compounds.

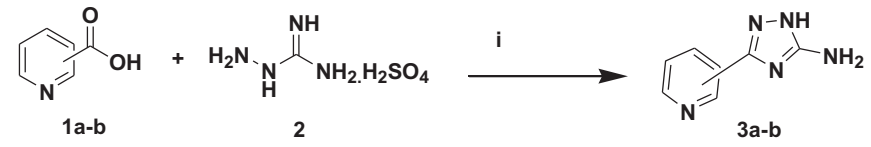

1,3 : a; pyridin-3-yl, b: pyridin-4-yl

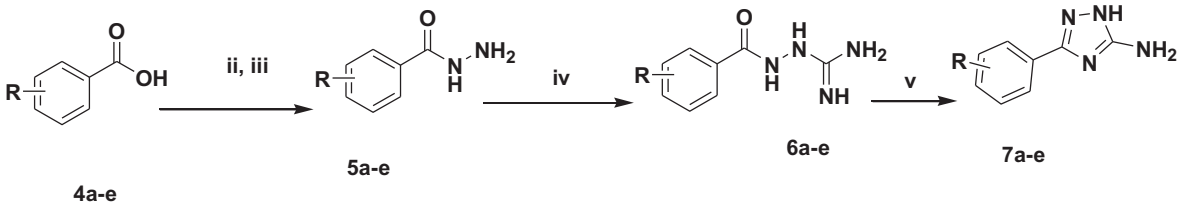

4, 5, 6, 7: a; R=H, b; R= 4-OCH_3, c; R= 3,4,5-tri (OCH_3), d; R= 3-Cl, e; R= 4-Cl

Reagents and reaction condition (i) Heating at 210°c, 2 h; (ii) H_2SO_4 / CH_3OH, reflux, 4-8 h; (iii) $NH_2NH_2.H_2O$, C_2H_5OH, reflux, 2-4 h; (iv) S-methylthiourea, NaOH, stirring, RT, 72 h; (v) water, reflux, 4 h

Scheme 1. Synthesis of the key intermediate **3a-b** and **7a-e**.

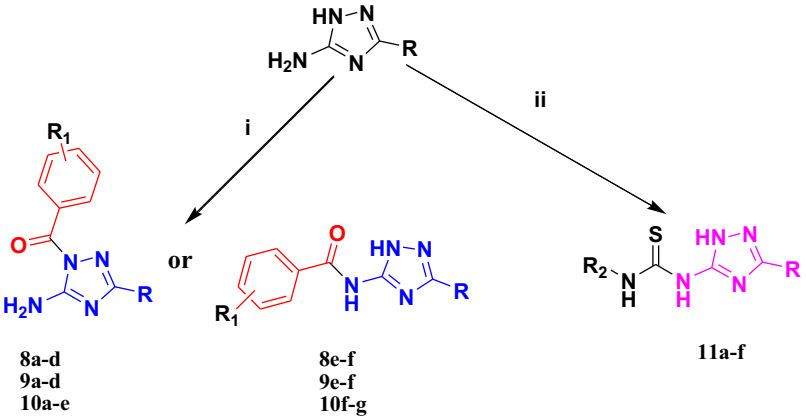

Reagents and reaction condition (i) Substituted benzoyl chloride, pyridine, stirring for 30 minutes at -5 °C, then at RT, 24 h; (ii) Substituted isothiocyanates, C_2H_5OH, stirring, RT, 3 h.

Compd. No.	R	R_1	Compd. No.		R_1	R_2
8a	C_6H_5	4-OCH_3	10a	C_6H_5	3,4,5-tri(OCH_3)	-
8b	3,4,5-tri(OCH_3) C_6H_2	4-OCH_3	10b	3,4,5-tri(OCH_3) C_6H_2-	3,4,5-tri(OCH_3)	-
8c	Pyridine-3-yl	4-OCH_3	10c	Pyridine-3-yl	3,4,5-tri(OCH_3)	-
8d	Pyridine-4-yl	4-OCH_3	10d	Pyridine-4-yl	3,4,5-tri(OCH_3)	-
8e	4-OCH_3-C_6H_4-	4-OCH_3	10e	4-Cl-C_6H_4-	3,4,5-tri(OCH_3)	-
8f	3-Cl-C_6H_4-	4-OCH_3	10f	4-OCH_3-C_6H_4-	3,4,5-tri(OCH_3)	-
9a	C_6H_5	3,4-di(OCH_3)	10g	3-Cl-C_6H_4-	3,4,5-tri(OCH_3)	-
9b	3,4,5-tri(OCH_3) C_6H_2	3,4-di(OCH_3)	11a	3,4,5-tri(OCH_3) C_6H_2-	-	C_6H_5
9c	Pyridine-3-yl	3,4-di(OCH_3)	11b	3,4,5-tri(OCH_3) C_6H_2-	-	C_2H_5
9d	Pyridine-4-yl	3,4-di(OCH_3)	11c	4-OCH_3-C_6H_4-	-	C_6H_5
9e	4-OCH_3-C_6H_4-	3,4-di(OCH_3)	11d	4-OCH_3-C_6H_4-	-	C_2H_5
9f	3-Cl-C_6H_4-	3,4-di(OCH_3)	11e	3-Cl-C_6H_4-	-	C_6H_5
			11f	3-Cl-C_6H_4-	-	C_2H_5

Scheme 2. Synthesis of the target compounds **8a-f**, **9a-f**, **10a-g** and **11a-f**.

IR spectra of compounds **10a-e** showed forked peak at 3110–3160 cm^{-1}due to NH_2 group, while compounds **10f-g** exhibited sharp peaks at 3390–3420 cm^{-1} due to NH gp of triazole. On the other hand, a characteristic intense peak appears at 3230–3245 cm^{-1} corresponding to presence of amidic NH. Furthermore, in compounds **10a-e** the carbonyl group CO-N appears in the region of 1685–1698 cm^{-1}, while in compounds **10f-g** CO-NH appears at the region of 1650–1655 cm^{-1}.

^{1}H NMR spectra of compounds **10a-e** characterized by the presence of a singlet signal at δ 7.85–7.96 ppm (2H) corresponding to NH_2 of triazole which totally disappeared in compounds **10f-g** which confirm that acylation occurs on NH_2 not on NH of triazole. On the other hand, singlet peak appears at δ 10.36–10.53 ppm corresponding to amidic CO-NH of amide, while the signal of NH-triazole appears at 10.40–10.65 ppm. In addition, the ^{1}H NMR of compounds **10a-g** showed a singlet peak at δ 7.27–7.63 ppm (2H) corresponding to aromatic protons. Appropriate signals for other aryl substituents were detected in the ^{1}H NMR spectra of compounds **10a-g.** ^{13}C NMR spectra of compounds **10a-g** exhibited some characteristic peaks at δ 56, 60 ppm corresponding to OCH3 gp, 159–165 ppm for C=O gp of amide and at δ 165–167 ppm corresponding to C=N group of triazole.

IR spectra of compounds **11a-f** showed significant peak at 3380–3450 cm^{-1} due to NH-triazole. In addition to significant sharp peaks appear at 3280–3410 cm^{-1} corresponding to NH gp of isothiocyanates and for amino-triazole, indicating that reaction occurs on terminal NH_2 not cyclic NH of triazole.

The ^{1}H NMR spectra of isothiocyanate derivatives **11a-f** showed characteristic singlet signals of NH at δ 8.06–10.43 ppm which are more downfield in phenyl derivatives 9.64–10.67 ppm. Moreover, compounds **11b, 11d** and **11f** exhibited triplet (CH_3) and quartet (CH_2) peaks in aliphatic regions at 1.05–1.09 ppm and 3.42–3.53 ppm, respectively indicating for ethyl group, while compounds **11a, 11c** and **11e** showed characteristic signals at 7.04–7.93 ppm

of phenyl group. Compounds **11a-f** showed singlet signals at 3.83 ppm corresponding to OCH_3 and at 3.72 and 3.84 ppm for 3,4,5-triOCH_3. ^{13}C NMR spectra of compound **11a-f** showed different significant peaks at δ 56 and 60 ppm related to triOCH_3 gp, 15 and 41 ppm for CH_2 and CH_3 of ethyl derivatives which disappear in case of phenyl derivatives.

2.2. Biology

2.2.1. Antiproliferative activity

For all triazole based compounds cell viability assay was carried out by using human mammary gland epithelial cell line (MCF-10A). All new synthetic compounds were treated with MCF-10A cells for 4 days and 3-(4,5-dimethylthiazol-2-yl)-2,5-diphenyltetrazolium bromide (MTT) assay was applied to gauge the viability of cells. All compounds were revealed to be nontoxic with the majority of them exhibiting more than 91% MCF-10A cell viability.

The new synthetic triazole containing compounds, prepared in this study, were assessed according to standard protocols for their *in vitro* antiproliferative activity against four human cancer cell lines including human pancreas cancer cell line (Panc-1), pancreatic carcinoma cells (PaCa-2), colon cancer cells (HT-29) and lung cancer cells (H-460) using the propidium iodide (PI) fluorescence assay. For comparison purposes Erlotinib, a drug used to treat non-small cell lung cancer, pancreatic cancer and several other types of cancer, was used as a standard cytotoxic drug [53,54]. GraphPad Prism software (GraphPad Software, San Diego, CA, USA) was used to calculate the median inhibition concentration (IC_{50}) for all compounds. All of IC_{50} values in micromolar (μM) are listed in (Table 1).

Five of the tested compounds (**8b, 8c, 8d, 10b** and **10e**) showed noteworthy antiproliferative effects with IC_{50} values < 2.0 μM. Compounds **10b** and **10e** showed almost comparable and very eminent anticancer activity against all cancer cell lines with IC_{50} ranging from 0.9 ± 0.2 to 2.2 ± 0.6 μM. Among these two compounds, **10b** showed more effects on other three cell lines as compared to lung cancer cells where growth inhibition was less (2.2 ± 0.6 μM) but still well as reference to most of other tested compounds. The synthetic free amino group containing triazole based compound **8b** demonstrated highest anticancer potential with IC_{50} of 0.2 ± 0.1 μM for Panc-1. Compounds **10b** and **10e** exhibited worth mentioning anticancer activity with IC_{50} 1.2 ± 0.6 μM and 0.9 ± 0.6 μM, respectively for HT-29 cells. The derivatives **8c** and **8d** also exhibited noteworthy inhibition of cancer cells**.** Among these new triazole based derivatives, compound **8b** exhibited very close cytotoxic effect to the standard against Panc-1 cell line. While some compounds have not been essentially convincing, their unambiguous activity against certain cell lines makes it more useful to develop as anti-cancer drugs. On the basis of IC_{50}, an exciting association was witnessed between the analogues in terms of their structural features. From the above mentioned results it is appears that most of the tested compounds bears free NH_2 group attached triazole were more effective than other derivatives with amide attached triazole in which the 5-amino was substituted either *N*-acyl or isothiocyanate. As shown in table 1, compound **10e** was more active than **10 g** while substitution pattern was same in both compounds and they differ only in backbone. Similar 1-(5-amino-[1,2,4]triazol-1-yl)ethanone containing compounds were reported by Romagnoli et al. and a new class of compounds that incorporated the structural motif of the 1-(3′,4′,5′-trimethoxtbenzoyl)-3-arylamino-5-amino-1,2,4-triazole molecular skeleton was synthesized and evaluated for their antiproliferative activity *in vitro*. Structure-activity relationships were explained with various substituents on the phenyl ring of the anilino moiety at the C-3 position of the 1,2,4-triazole ring. The best results for inhibition of cancer cell growth were obtained with the *p*-Me, *m,p*-diMe, and *p*-Et phenyl derivatives. This study supports our results as similar substitution pattern in newly synthesized triazole based compounds showed very potent effects against cancer cell lines [55].

Trimethoxy substitution on triazole attached aromatic ring (**8b**) exhibited additional activity as compared to unsubstituted phenyl ring containing compounds (**8a**). Similarly synthetic compound **9b**

Table 1
Antiproliferative activities of synthetic compounds.

	Antiproliferative activity IC_{50} ± SEM (μM)				
No.	Code	Panc-1	PaCa-2	HT-29	H-460
1	**8a**	2.5 ± 1.1	1.5 ± 0.7	1.9 ± 1.6	1.6 ± 0.7
2	**8b**	0.2 ± 0.1	0.8 ± 0.5	1.6 ± 0.4	1.3 ± 0.2
3	**8c**	1.5 ± 0.9	1.0 ± 0.1	1.4 ± 0.7	1.7 ± 0.5
4	**8d**	1.9 ± 1.5	1.3 ± 0.9	1.7 ± 0.9	1.6 ± 0.7
5	**8e**	7.2 ± 1.5	8.4 ± 1.4	9.9 ± 2.7	8.2 ± 2.3
6	**8f**	7.4 ± 1.5	7.6 ± 2.7	6.5 ± 2.4	7.9 ± 1.6
7	**9a**	7.8 ± 1.9	9.4 ± 2.1	6.5 ± 2.4	7.0 ± 2.1
8	**9b**	4.1 ± 1.2	5.3 ± 1.2	3.1 ± 1.4	6.9 ± 1.6
9	**9c**	5.5 ± 2.5	5.9 ± 3.0	6.7 ± 2.4	6.4 ± 1.1
10	**9d**	5.8 ± 2.4	6.1 ± 2.4	6.9 ± 1.7	7.9 ± 1.5
11	**9e**	9.4 ± 2.1	11.6 ± 1.7	11.0 ± 1.5	12.9 ± 1.9
12	**9f**	11.9 ± 2.3	14.2 ± 3.5	16.9 ± 2.9	13.5 ± 2.8
13	**10a**	4.5 ± 1.4	5.8 ± 2.2	8.7 ± 1.1	9.0 ± 1.5
14	**10b**	1.3 ± 0.9	1.7 ± 0.9	1.2 ± 0.6	2.2 ± 0.6
15	**10c**	3.5 ± 1.9	2.9 ± 1.5	2.9 ± 1.5	3.2 ± 1.0
16	**10d**	3.2 ± 1.2	2.9 ± 0.8	3.1 ± 2.0	2.9 ± 0.8
17	**10e**	1.0 ± 0.9	1.7 ± 1.0	0.9 ± 0.6	0.9 ± 0.2
18	**10f**	7.1 ± 1.3	7.5 ± 1.5	9.2 ± 2.7	9.9 ± 1.5
19	**10g**	2.6 ± 1.4	3.0 ± 0.8	2.0 ± 1.1	2.8 ± 1.5
20	**11a**	4.2 ± 0.8	6.9 ± 2.4	4.7 ± 1.8	5.8 ± 3.5
21	**11b**	5.5 ± 1.5	5.2 ± 2.7	4.9 ± 0.6	4.1 ± 1.5
22	**11c**	3.2 ± 1.9	2.7 ± 0.5	4.3 ± 0.5	2.6 ± 0.3
23	**11d**	4.8 ± 0.7	6.6 ± 1.5	7.2 ± 1.6	6.1 ± 2.9
24	**11e**	5.9 ± 2.8	5.0 ± 1.8	4.2 ± 1.9	4.9 ± 1.6
25	**11f**	7.4 ± 2.9	5.7 ± 1.6	7.9 ± 1.2	5.9 ± 0.9
Erlotinib		0.04 ± 0.02	0.02 ± 0.02	0.04 ± 0.01	0.02 ± 0.02

Panc-1(pancreas cancer cell line); PaCa-2 (pancreatic carcinoma cell line); HT-29 (colon cancer cell line); H-460 (lung cancer cell line).

Table 2
Effects of compounds **(8a, 8b, 8c, 8d, 10b, 10e,** and **10g)** on Tubulin Polymerization, EGFR and $BRAF^{V600E}$.

Comp.	(Tubulin) Effect (arbitrary units)	EGFR inhibition IC_{50} ± SEM (μM)	BRAF inhibition IC_{50} ± SEM (μM)
8a	1240 ± 206	8.9 ± 3.7	2.0 ± 1.2
8b	1150 ± 177	9.4 ± 1.5	2.7 ± 0.7
8c	957 ± 120	3.6 ± 0.8	1.9 ± 0.8
8d	872 ± 155	4.6 ± 1.7	1.8 ± 0.7
10b	2015 ± 138	6.5 ± 1.2	5.1 ± 2.0
10e	1502 ± 210	5.5 ± 2.1	5.8 ± 1.5
10g	1920 ± 272	7.4 ± 2.2	4.0 ± 1.3
Erlotinib	–	0.07 ± 0.03	0.04 ± 0.03
DPBS	2880 ± 237	–	–
Vincristine	722 ± 249	–	–
Docetaxel	4735 ± 217	–	–

exhibited more inhibition of cancer cell growth as compared to **9a**. Replacement of triazole attached methoxy substituted aromatic ring with pyridine increased the antiproliferative effects (**8c, 9c, 10c**). Halogen attachment at position **4** of the triazole attached aromatic ring (**10e**) exhibited more effects than attachment at position **3** (**10 g**).

On the other hand, substitution arrangement on carbonyl attached phenyl ring also showed very interesting biological relationship as mono methoxy substituted derivatives (**8b**) were found **20** folds more potent than dimethoxy containing compounds (**9b**). Trimethoxy existence (**10b**) showed noticeable activity that was much better to dimethoxy containing compounds (**9b**) but less as compared to monomethoxy substitution pattern (**8b**).

Substituted phenyl attached triazoles with and without amide linkage has been reported previously and a structure-activity relationship (SAR) study of the *N*-((3-chloro-2-hydroxy-5-nitrophenyl) carbamothioyl)benzamide series revealed that increased liver microsomal stability and toxicity towards cancer cells could be attained by replacing the central thiourea unit with the 1,2,3-triazole heterocycle unit. These derivatives not only enhanced the cell death, but also concealed the cell migration and invasion through the attenuation of actin cytoskeleton remodelling. Consistently, most active derivative also showed significantly increased activity in the cell migration assay [56,57]. Further to the above-mentioned antiproliferative activity, compounds **10b, 10e, 10 g, 8a, 8b, 8c** and **8d** were selected for mechanistic study against Tubulin, EGFR and $BRAF^{V600E}$ kinase enzymes.

2.2.2. Tubulin inhibitory activity

The effect of new synthetic compounds on tubulin polymerization was summarized in Table 2**.** Most of the tested compounds inhibited the assembly of tubulin, with compounds **8c** and **8d** proving to be the strongest inhibitors. On the other hand, compounds **10b** and **10 g** did not inhibit the assembly of tubulin suggesting a different mechanism for the observed cytotoxicity of these compounds rather than tubulin inhibition.

2.2.3. EGFR inhibitory activity

Table 2 shows the findings of EGFR-TK assay performed to evaluate the EGFR inhibitory potential of the tested compounds **8a, 8b, 8c**, **8d, 10b, 10e** and **10 g,** moderate EGFR inhibition was shown by all of the tested compounds with IC_{50} of 3.6–9.4 μM. According to Table 2**,** compounds **8c** and **8d** were discovered to be most active and they inhibited EGFR with IC_{50} of 3.6 and 4.6 μM, respectively. The activity of compounds **8c** and **8d** were found to be enhanced by the presence of 3-pyridyl *or* 4-pyridyl moiety. Although, they showed moderate activity against EGFR inhibition nonetheless were found to be potent inhibitors of tubulin assembly.

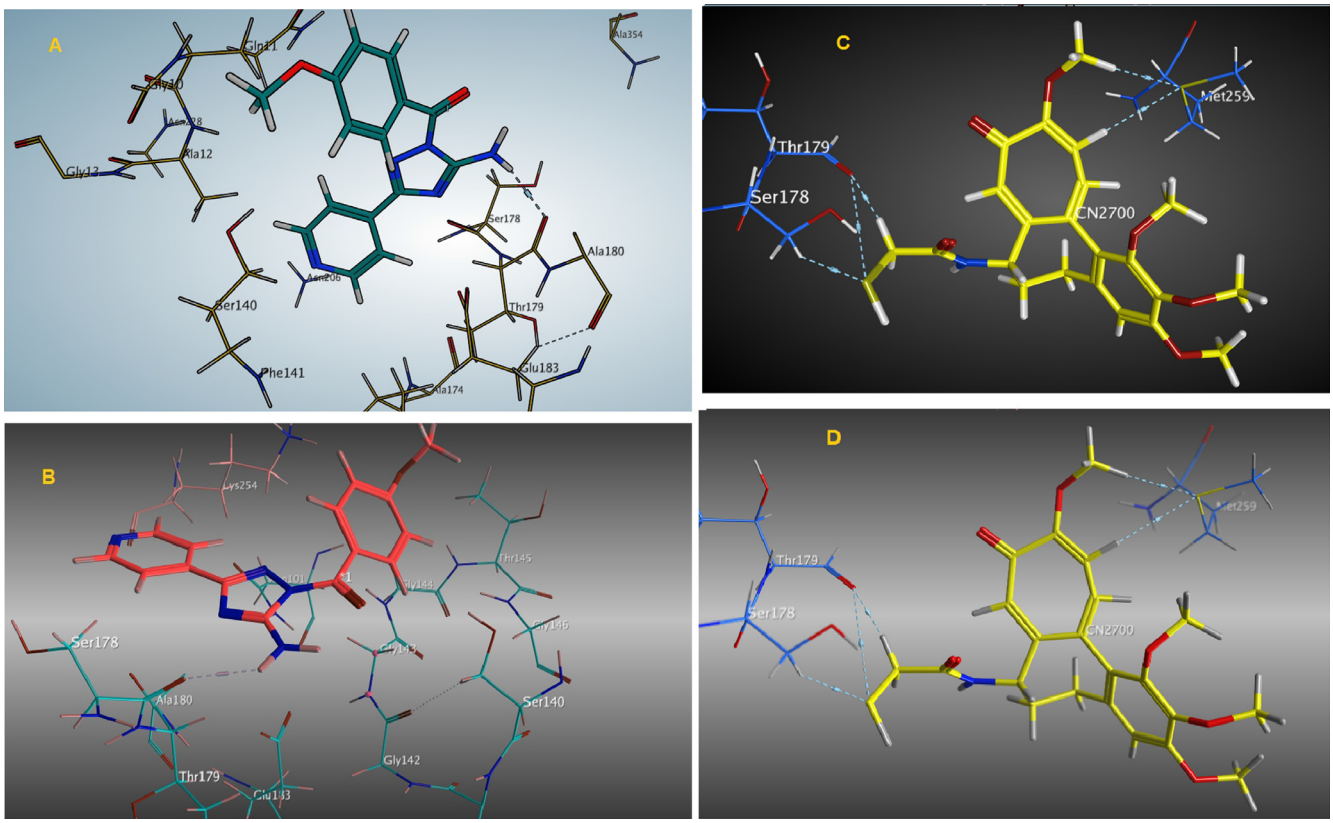

Fig. 3. (A and B) 3D overlay of the top docked poses **8d** in addition to the co-crystallized ligand colchicine into the tubulin binding pocket (PDB code: isa0); (C and D) 3D overlay of the top docked colchicine as a co-crystallized ligand into tubulin active site.

2.2.4. $BRAF^{V600E}$ inhibitory activity

The potential of the newly synthesized compounds against $BRAF^{V600E}$ was tested using an *in vitro* experiment. Table 2 shows the IC_{50} of the tested compounds ranging from 1.8 to 5.8 μM. All 5-amino1,2,4-triazole-based compounds **(8a, 8b, 8c**, **8d, 10b, 10e** and **10 g)** strongly inhibited $BRAF^{V600E}$. Compounds **8c** and **8d** showed almost same BRAF inhibitory activity and were discovered to be potent inhibitors of cancer cell proliferation and were also observed to be strong tubulin inhibitors. The results from this study show that the tested compounds have remarkable anticancer activity and they also inhibit BRAF enzyme efficiently.

2.3. Molecular modeling study

This study was performed to gain some structural insights into the potential binding patterns and possible interactions of the most active 1,2,4-triazole derivatives, **8c** and **8d**, inside the active sites of Tubulin using MOE (Molecular Operating Environment) software. The 3D crystal structures of Tubulin (PDB ID: 1sa0), in complex with colchicine, was used for this docking simulation study [58,59]. Meanwhile, the possible interactions and ligands orientation were investigated. The overlay of the top docking poses tubulin proteins binding pockets were presented in Fig. 3 where the poses **8c** and **8d** showed good shape complementarily with the binding active sites of both proteins.

Analysis of the docking results revealed that the most active compound **8c** and **8d** against tubulin fit nicely inside the ATP-active site engaging in two hydrogen bonds with **Thr 179** and **Ser 178** residues Fig. 4(A) and (B). Moreover, the triazole core was extended towards the hinge region forming hydrophobic interactions with **Lys 254**, **Ala 12**, **Tyr 224** and **Leu 248** amino acids. Interestingly, both compounds **8c** and **8d** adopted the same orientation inside the active pocket of Tubulin owing to the high similarity between the two structures. However, compound **8d** was protruded towards the hinge region to some extent more than compound **8c** due to the difference of the pyridinyl group. Also, amide and free amino moiety formed a hydrogen bond with the Lys 254 residue and was involved as well in another hydrogen bond interaction with Asn 101 amino acid. It is worth noting that there is a remarkable similarity between the common binding mode of the two docked ligands **8c** and **8d** with that of colchicine, Fig. 4(C). The mercapto moiety in colchicine formed two hydrogen bonds with **Ser178** and **Thr179** residues like free amino group in compounds **8c** and **8d**. This apparent similarity between the binding modes of the newly synthesized compounds and the native ligand may greatly contribute to their remarkable potency against Tubulin.

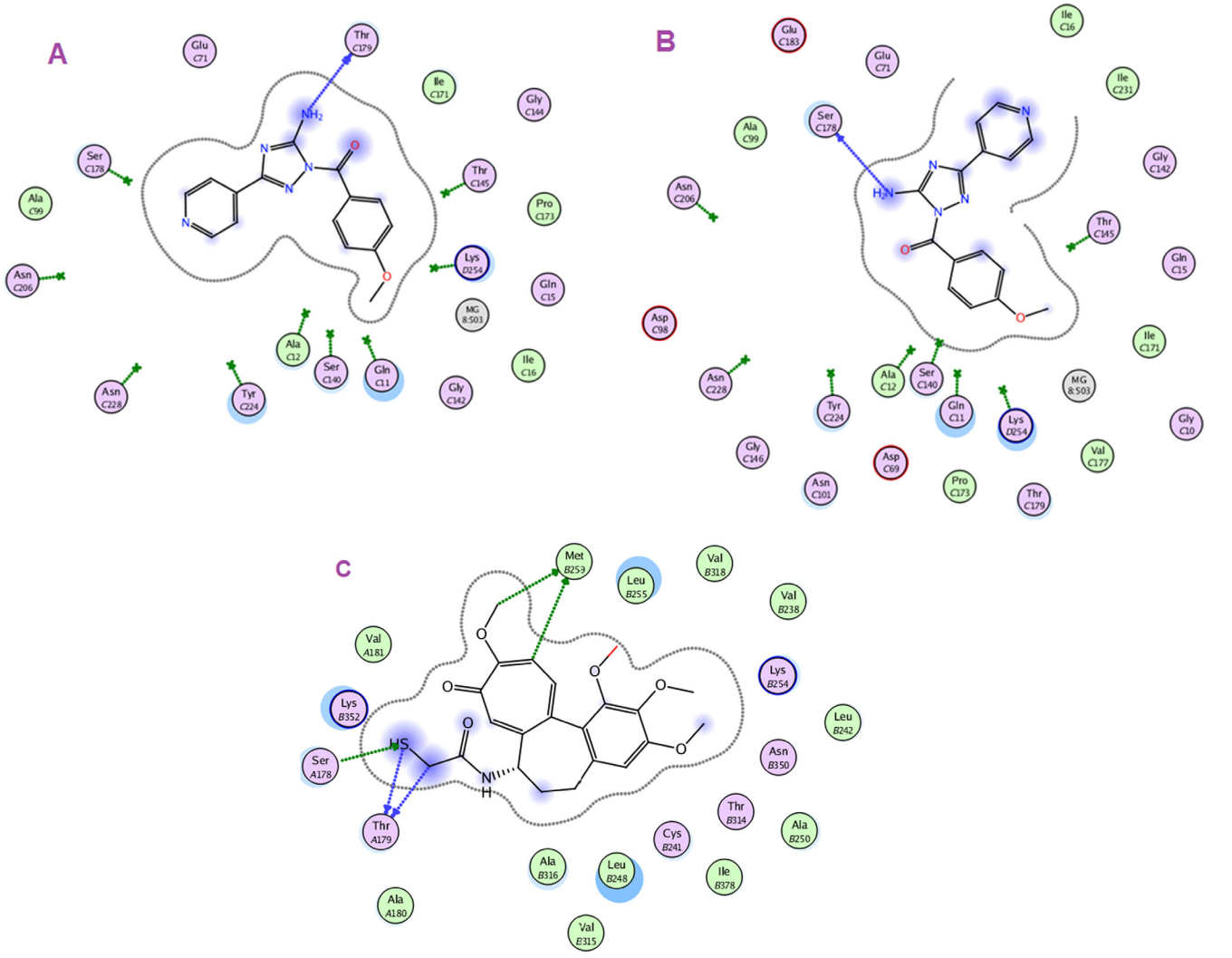

Fig. 4. (A and B) Docking and binding pattern of compound **8d** into ATP-active site of tubulin (PDB code: isa0). (C) Docking and binding pattern of colchicine into ATP-active site of tubulin.

3. Conclusion

In this study, a new set of compounds bearing 1,2,4-triazole core was synthesized and evaluated for their anticancer activity against a panel of cancer cell lines. The inhibitory activity of the most active compounds **8a, 8b, 8c, 8d, 10b, 10e,** and **10 g** in MTT assay were examined against three known anticancer targets including EGFR, BRAF and tubulin. The results revealed that compounds **8c** and **8d** showed a strong Tubulin inhibition. Moreover, **8c** showed the best EGFR inhibition with IC_{50} = 3.6 μM.

4. Experimental

4.1. Chemistry

Reactions were monitored by TLC analysis using Merck 9385 pre-coated aluminum plate silica gel (Kieselgel 60) with F_{254} indicator thin layer plates. Melting points were determined on Stuart electrothermal melting point apparatus and were uncorrected. IR spectra were recorded as KBr disks on a Shimadzu S8400 IR spectrophotometer. ^{1}H NMR spectra were carried out on 400 MHz Brucker spectrometer, using TMS as an internal reference. Chemical shift (δ) values are given in parts per million (ppm) relative to $CDCl_3$ (7.29) or DMSO d_6 (2.5) and coupling constants (J) in Hertz. Splitting patterns are designated as follows: s, singlet; d, doublet; t, triplet; q, quartet; dd, doublet of doublet; m, multiplet. High resolution mass spectrometric data were obtained using MicroTOF-Q mass spectrometer (Bruker), Malaysia. Compounds **3a-b** and **7a-e** were prepared according to reported procedures.

4.2. General method for Synthesis of (5-amino-3-(hetero)aroyl-1H-1,2,4-triazol-1-yl) (substituted phenyl) methanone (*8a-f*, *9a-f* and *10a-g*)

Substituted benzoyl chloride (1.1 mmol) was added in small portions to a stirred solution of the appropriate compounds **3a-b** or **7a-e** (1 mmol) in dry pyridine (10 mL) cooled to −5 °C. The reaction mixture was kept for 30 min at −5 °C and then stirred overnight at room temperature. Reaction mixture was then poured into ice; the obtained precipitate was filtered off, dried and recrystallized from ethanol to afford compounds **8a-f, 9a-f** and **10a-g**.

4.2.1. (5-Amino-3-phenyl-1H-1,2,4-triazol-1-yl)(4-methoxyphenyl) methanone (*8a*)

White powder (0.19 g, 67% yield), m.p. 178–180 °C, IR (KBr) υ_{max} (cm^{-1}) 3140 (NH_2), 1690 (C=O); ^{1}H NMR (400 MHz, DMSO d_6) δ (ppm): 3.86 (s, 3H, OCH_3), 7.12 (d, 2H, *J* = 8.8 Hz, OCH_3-Ar-H), 7.48–7.50 (m, 3H, Ar-H), 7.88–7.99 (m, 4H, Ar-H + NH_2), 8.26–8.30 (m, 2H, Ar-H); ^{13}C NMR (100 MHz, DMSO d_6) δ (ppm): 56.08, 114.06, 124.17, 126.89, 129.18, 129.65, 130.76, 131.80, 134.14, 159.34, 163.69, 166.99; HRMS (ESI) *m*/*z*: $[M+Na]^+$ calc = 317.1014; found 317.1016 $C_{16}H_{14}N_4O_2$.

4.2.2. (5-Amino-3-(3,4,5-trimethoxyphenyl)-1H-1,2,4-triazol-1-yl)(4-methoxyphenyl)methanone (*8b*)

White powder (0.21 g, 55% yield), m.p. 189–191 °C, IR (KBr) υ_{max} (cm^{-1}) 3150 (NH_2), 1695 (C=O); ^{1}H NMR (400 MHz, DMSO d_6) δ (ppm): 3.72 (s, 3H, OCH_3), 3.85 (s, 6H, $2OCH_3$), 3.89 (s, 3H, OCH_3), 7.14 (d, 2H, *J* = 8.8 Hz, OCH_3-Ar-H), 7.26 (s, 2H, NH_2), 7.79 (s, 2H, Ar-H), 8.29 (d, 2H, *J* = 8.8 Hz, Ar-H); ^{13}C NMR (100 MHz, DMSO d_6) δ (ppm): 55.88, 56.09, 56.50, 60.61, 104.21, 105.46, 114.07, 126.11, 134.15, 140.87, 153.50, 159.49, 163.69, 166.94; HRMS (ESI) *m*/*z*: $[M+H]^+$ calc = 385.1512; found 385.1520 for $C_{19}H_{20}N_4O_5$.

4.2.3. (5-Amino-3-(pyridin-3-yl)-1H-1,2,4-triazol-1-yl)(4-methoxyphenyl)methanone (*8c*)

White powder (0.22 g, 75% yield), m.p. 204–206 °C, IR (KBr) υ_{max} (cm^{-1}) 3110 (NH_2), 1690 (C=O); ^{1}H NMR (400 MHz, DMSO d_6) δ (ppm): 3.89 (s, 3H, OCH_3), 7.13 (d, 2H, *J* = 8.8 Hz, Ar-H), 7.51–7.54 (m, 1H, Het-H), 7.88 (s, 2H, NH_2), 8.27–8.30 (m, 3H, Ar-H +Het-H), 8.67–8.67 (d, 1H, *J* = 4 Hz, Het-H), 9.14 (s, 1H, Het-H); ^{13}C NMR (100 MHz, DMSO d_6) δ)ppm): 56.07, 114.08, 124.02, 124.41, 126.55, 134.19, 134.29, 147.86, 151.29, 157.88, 159.65, 163.74, 167.01; HRMS (ESI) *m*/*z*: $[M+H]^+$ calc = 296.1147; found 296.1157 for $C_{15}H_{13}N_5O_2$.

4.2.4. (5-Amino-3-(pyridin-4-yl)-1H-1,2,4-triazol-1-yl)(4-methoxyphenyl)methanone (*8d*)

White powder (0.21 g, 72% yield), m.p. 236–238 °C, IR (KBr) υ_{max} (cm^{-1}) 3120 (NH_2), 1690 (C=O); ^{1}H NMR (400 MHz, DMSO d_6) δ (ppm): 3.88 (s, 3H, OCH_3), 7.13 (d, 2H, *J* = 8.8 Hz, Ar-H), 7.87 (d, 2H, *J* = 8.4 Hz, Het-H), 7.88 (s, 2H, NH_2), 8.26 (d, 2H, *J* = 8.8 Hz, Ar-H), 8.71 (d, 2H, *J* = 8.4 Hz, Het-H); ^{13}C NMR (100 MHz, DMSO d_6) δ (ppm): 56.09, 114.09, 120.97, 123.96, 134.19, 138.01, 150.72, 158.03, 159.79, 163.79, 167.04; HRMS (ESI) *m*/*z*: $[M+H]^+$ calc = 296.1147; found 296.1159 for $C_{15}H_{13}N_5O_2$.

4.2.5. 4-Methoxy-N-(5-(4-methoxyphenyl)-2H-1,2,4-triazol-3-yl) benzamide (*8e*)

White powder (0.22 g, 70% yield), m.p. 232–234 °C, IR (KBr) υ_{max} (cm^{-1}) 3400, 3250 (NH, NH-amide), 1635 (C=O); ^{1}H NMR (400 MHz, DMSO d_6) δ (ppm): 3.84 (s, 6H, $2OCH_3$), 7.06 (d, 4H, *J* = 8.8 Hz, Ar-H), 7.92 (d, 4H, *J* = 8.8 Hz, Ar-H), 10.29 (s, 2H, 2NH); ^{13}C NMR (100 MHz, DMSO d_6) δ (ppm): 55.87, 114.19, 125.27, 129.80, 162.46, 165.87; HRMS (ESI) *m*/*z*: $[M-H]^-$ calc = 323.1222; found 323.1013 for $C_{17}H_{16}N_4O_3$.

4.2.6. N-(5-(3-Chlorophenyl)-2H-1,2,4-triazol-3-yl)-4-methoxybenzamide (8f)

White powder (0.26 g, 80% yield), m.p. 214–216 °C, IR (KBr) υ_{max} (cm^{-1}) 3390, 3230 (NH, NH-amide), 1640 (C=O); ^{1}H NMR (400 MHz, DMSO d_6) δ (ppm): 3.84 (s, 3H, OCH_3), 7.06 (d, 2H, *J* = 8.8 Hz, Ar-H), 7.56–7.60 (m, 1H, Ar-H), 7.69 (d, 1H, *J* = 8.0 Hz, Ar-H), 7.80–7.91 (m, 2H, Ar-H), 7.95 (d, 2H, *J* = 8.8 Hz, Ar-H), 10.42 (s, 1H, CO-NH), 10.58 (s, 1H, NH); ^{13}CNMR (100 MHz, DMSO d_6) δ (ppm): 55.87, 114.24, 124.91, 126.62, 127.68, 129.87, 130.15, 131.12, 131.80, 132.24, 133.85, 134.96, 162.58, 165.21, 165.97; HRMS (ESI) *m*/*z*: $[M-H]^-$ calc = 327.0649; found 327.0507 for $C_{16}H_{12}ClN_4O_2$).

4.2.7. (5-Amino-3-phenyl-1H-1,2,4-triazol-1-yl)(3,4-dimethoxyphenyl) methanone (*9a*)

White powder (0.21 g, 66.4% yield), m.p. 203–205 °C, IR (KBr) υ_{max} (cm^{-1}) 3130 (NH_2), 1695 (C=O); ^{1}H NMR (400 MHz, DMSO d_6) δ (ppm): 3.84 (s, 3H, OCH_3), 3.87 (s, 3H, OCH_3), 7.13–7.15 (m, 1H, Ar-H), 7.47–7.51 (m, 3H, Ar-H), 7.81 (s, 2H, NH_2), 7.89 (s, 1H, Ar-H), 8.00–8.06 (m, 3H, Ar-H); ^{13}C NMR (100 MHz, DMSO d_6) δ (ppm): 56.10, 56.23, 111.18, 111.56, 114.66, 123.96, 125.82, 126.52, 126.81, 128.88, 129.19, 130.52, 130.66, 148.78, 153.58, 159.65, 159.85, 166.89; HRMS (ESI) *m*/*z*: $[M+Na]^+$ calc = 347.1120; found 347.1123 for $C_{17}H_{16}N_4O_3$.

4.2.8. (5-Amino-3-(3,4,5-trimethoxyphenyl)-1H-1,2,4-triazol-1-yl)(3,4-dimethoxyphenyl) methanone (*9b*)

White powder (0.21 g, 52% yield), m.p. 244–246 °C, (KBr) υ_{max} (cm^{-1}) 3150 (NH_2), 1695 (C=O), 1610 (C=N); ^{1}HNMR (400 MHz, DMSO d_6) δ (ppm): 3.72 (s, 3H, OCH_3), 3.81 (s, 3H, OCH_3), 3.83 (s, 6H, $2OCH_3$), 3.89 (s, 6H, $2OCH_3$), 7.16 (d, 1H, *J* = 8.4 Hz, OCH_3-Ar-H), 7.26 (s, 2H, NH_2), 7.82 (s, 2H, Ar-H), 7.95 (d, 1H, *J* = 8.4 Hz,

OCH_3-Ar-H), 8.09 (s, 1H, Ar-H); ^{13}C NMR (100 MHz, DMSO d_6) δ = 56, 60, 103, 109, 125, 126, 139, 142, 152, 153, 159, 166; HRMS (ESI) m/z: $[M+NH_4]^+$ calc = 432.1883; found = 432.1908.

*4.2.9. (5-Amino-3-(pyridin-3-yl)-1H-1,2,4-triazol-1-yl)(3,4-dimethoxyphenyl)methanone (**9c**)*

White powder (0.22 g, 68% yield), m.p. 247–249 °C, IR (KBr) υ_{max} (cm^{-1}) 3115 (NH_2), 1685 (C=O); ^1H NMR (400 MHz, DMSO d_6) δ (ppm): 3.85 (s, 3H, OCH_3), 3.89 (s, 3H, OCH_3), 7.16 (d, 1H, J = 8.8 Hz, Ar-H), 7.52–7.55 (m, 1H, Het-H), 7.86 (s, 1H, Ar-H), 7.89 (s, 2H, NH_2), 8.00–8.02 (m, 1H, Ar-H), 8.28 (d, 1H, J = 8.0 Hz, Het-H), 8.66–8.67 (m, 1H, Het-H), 9.14 (s, 1H, Het-H); ^{13}C NMR (100 MHz, DMSO d_6) δ (ppm): 56.02, 56.24, 111.23, 114.62, 123.79, 124.41, 126.59, 134.17, 134.60, 147.84, 148.29, 151.29, 153.65, 157.87, 159.74, 166.84; Elemental analysis for $C_{16}H_{15}N_5O_3$ (324.1), Calculated; C, 59.07; H, 4.65; N, 21.53; Found C, 59.29; H, 4.80; N, 21.87.

*4.2.10. (5-Amino-3-(pyridin-4-yl)-1H-1,2,4-triazol-1-yl)(3,4-dimethoxyphenyl)methanone (**9d**)*

White powder (0.23 g, 71% yield), m.p. 193–195 °C, IR (KBr) υ_{max} (cm^{-1}) 3120 (NH_2), 1686 (C=O); ^1H NMR (400 MHz, DMSO d_6) δ (ppm): 3.79 (s, 3H, OCH_3), 3.81 (s, 3H, OCH_3), 7.04 (d, 1H, J = 8.4 Hz, Ar-H), 7.42–7.44 (m, 1H, Ar-H), 7.54–7.57 (m, 1H, Ar-H), 8.07–8.09 (m, 3H, Ar-H+NH_2), 8.74–8.76 (m, 3H, Ar-H); ^{13}C NMR (100 MHz, DMSO d_6) δ (ppm): 55.89, 56.10, 111.42, 112.30, 121.39, 123.38, 123.69, 143.50, 146.29, 148.82, 153.31, 155.31, 158.41, 167.58; Elemental analysis for $C_{16}H_{15}N_5O_3$ (324.1), Calculated; C, 59.07; H, 4.65; N, 21.53; Found C, 59.34; H, 4.77; N, 21.45.

*4.2.11. 3,4-Dimethoxy-N-(5-(4-methoxyphenyl)–2H-1,2,4-triazol-3-yl)benzamide (**9e**)*

White powder (0.23 g, 65.7% yield), m.p. 194–196 °C, IR (KBr) υ_{max} (cm^{-1}) 3415, 3255 (NH, NH-amide), 1650 (C=O); ^1H NMR (400 MHz, DMSO d_6) δ (ppm): 3.83 (s, 3H, OCH_3), 3.84 (s, 6H, $2OCH_3$), 7.06 (d, 2H, J = 8.4 Hz, Ar-H), 7.09 (s, 1H, Ar-H), 7.53–7.59 (m, 2H, Ar-H), 7.92 (d, 2H, J = 8.8 Hz, Ar-H), 10.31 (s, 2H, NH); ^{13}C NMR (100 MHz, DMSO d_6) δ (ppm): 55.86, 56.03, 56.09, 111.10, 111.50, 114.20, 121.36, 125.24, 125.27, 129.81, 148.78, 151.60, 152.16, 162.47, 165.19; HRMS (ESI) m/z: $[M-H]^-$ calc = 353.1328; found 353.1119 for $C_{18}H_{18}N_4O_4$.

*4.2.12. N-(5-(3-Chlorophenyl)–2H-1,2,4-triazol-3-yl)-3,4-dimethoxybenzamide (**9f**)*

White powder (0.25 g, 69% yield), m.p. 194–196 °C, IR (KBr) υ_{max} (cm^{-1}) 3395, 3235 (NH, NH-amide), 1645 (C=O); ^1H NMR (400 MHz, DMSO d_6) δ (ppm): 3.84 (s, 3H, OCH_3), 3.86 (s, 3H, OCH_3), 7.09 (d, 1H, J = 8.0 Hz, Ar-H), 7.53 (s, 1H, Ar-H), 7.57–7.60 (m, 2H, Ar-H),), 7.69 (d, 1H, J = 8.8 Hz, Ar-H), 7.90 (d, 1H, J = 8.8 Hz, Ar-H), 7.96 (s, 1H, Ar-H), 10.55 (s, 2H, NH); ^{13}C NMR (100 MHz, DMSO d_6) δ (ppm): 56.04, 56.10, 111.10, 111.52, 121.42, 124.98, 125.20, 126.69, 127.71, 131.10, 132.20, 133.85, 135.08, 148.81, 152.28, 165.07, 165.78; HRMS (ESI) m/z: $[M-H]^-$ calc = 357.0833; found 357.0817 for $C_{17}H_{15}ClN_4O_3$.

*4.2.13. (5-Amino-3-phenyl-1H-1,2,4-triazol-1-yl)(3,4,5-trimethoxyphenyl)methanone (**10a**)*

White powder (0.24 g, 66.4% yield), m.p. 231–233 °C, IR (KBr) υ_{max} (cm^{-1}) 3145 (NH_2), 1698 (C=O); ^1H NMR (400 MHz, DMSO d_6) δ (ppm): 3.81 (s, 3H, OCH_3), 3.87 (s, 6H, $2OCH_3$), 7.48–7.51 (m, 3H, Ar-H), 7.63 (s, 2H, Ar-H),7.85 (s, 2H, NH_2), 7.97–8.00 (m, 2H, Ar-H); ^{13}C NMR (100 MHz, DMSO d_6) δ (ppm): 56.57, 60.73, 107.02, 109.54, 126.01, 126.81, 126.99, 129.07, 129.28, 130.62, 142.22, 152.59, 159.65, 160.01, 166.80; HRMS (ESI) m/z: $[M+H]^+$ calc = 355.1406; found 355.1413 for $C_{18}H_{18}N_4O_4$.

*4.2.14. (5-Amino-3-(3,4,5-trimethoxyphenyl)-1H-1,2,4-triazol-1-yl)(3,4,5-trimethoxyphenyl) methanone (**10b**)*

White powder (0.23 g, 52% yield), m.p. 198–200 °C, IR (KBr) υ_{max} (cm^{-1}) 3160 (NH_2), 1698 (C=O); ^1H NMR (400 MHz, DMSO d_6) δ (ppm): 3.72 (s, 3H, OCH_3), 3.81 (s, 3H, OCH_3), 3.83 (s, 6H, $2OCH_3$), 3.89 (s, 6H, $2OCH_3$), 7.28 (s, 2H, Ar-H), 7.75 (s, 2H, Ar-H), 7.89 (s, 2H, NH_2); ^{13}C NMR (100 MHz, DMSO d_6) δ (ppm): 56.17, 56.44, 60.59, 60.74, 103.81, 109.76, 125.95, 126.66, 139.57, 142.35, 152.58, 153.50, 159.69, 159.81, 166.48; HRMS (ESI) m/z: $[M+H]^+$ calc = 445.1723; found 445.1734 for $C_{21}H_{24}N_4O_7$.

*4.2.15. (5-Amino-3-(pyridin-3-yl)-1H-1,2,4-triazol-1-yl)(3,4,5-trimethoxyphenyl)methanone (**10c**)*

White powder (0.24 g, 68% yield), m.p. 229–231 °C, IR (KBr) υ_{max} (cm^{-1}) 3120 (NH_2), 1690 (C=O); ^1H NMR (400 MHz, DMSO d_6) δ (ppm): 3.80 (s, 3H, OCH_3), 3.89 (s, 6H, $2OCH_3$), 7.52–7.55 (m, 1H, Het-H), 7.61 (s, 2H, Ar-H), 7.94 (s, 2H, NH_2), 8.27–8.30 (m, 1H, Het-H), 8.66–8.68 (m, 1H, Het-H), 9.13 (s, 1H, Het-H); ^{13}C NMR (100 MHz, DMSO d_6) δ (ppm): 56.39, 60.72, 107.00, 109.51, 124.56, 126.84, 133.56, 142.29, 147.73, 149.32, 153.11, 158.01, 159.72, 166.99; HRMS (ESI) m/z: $[M+H]^+$ calc = 356.1359; found 356.1357 for $C_{17}H_{17}N_5O_4$.

*4.2.16. (5-Amino-3-(pyridin-4-yl)-1H-1,2,4-triazol-1-yl)(3,4,5-trimethoxyphenyl)methanone (**10d**)*

White powder (0.25 g, 71% yield), m.p. 234–236 °C, IR (KBr) υ_{max} (cm^{-1}) 3125 (NH_2), 1690 (C=O); ^1H NMR (400 MHz, DMSO d_6) δ (ppm): 3.81 (s, 3H, OCH_3), 3.87 (s, 6H, $2OCH_3$), 7.58 (s, 2H, Ar-H), 7.89 (d, 2H, J = 8.4 Hz, Het-H), 7.96 (s, 2H, NH_2), 8.72 (d, 2H, J = 8.4 Hz, Het-H); ^{13}C NMR (100 MHz, DMSO d_6) δ (ppm): 56.60, 60.73, 109.50, 121.06, 125.21, 138.39, 142.33, 150.45, 152.62, 158.05, 159.83, 167.09; HRMS (ESI) m/z: $[M+H]^+$ calc = 356.1359; found 356.1367 for $C_{17}H_{17}N_5O_4$.

*4.2.17. (5-Amino-3-(4-chlorophenyl)-1H-1,2,4-triazol-1-yl)(3,4,5-trimethoxyphenyl)methanone (**10e**)*

White powder (0.24 g, 63% yield), m.p. 196–198 °C, IR (KBr) υ_{max} (cm^{-1}) 3110 (NH_2), 1685 (C=O); ^1H NMR (400 MHz, DMSO d_6) δ (ppm): 3.80 (s, 3H, OCH_3), 3.88 (s, 6H, $2OCH_3$), 7.55 (d, 2H, J = 8.4 Hz, Ar-H), 7.59 (s, 2H, Ar-H), 7.88 (s, 2H, NH_2), 7.97 (d, 2H, J = 8.4 Hz, Ar-H); ^{13}C NMR (100 MHz, DMSO d_6) δ (ppm): 56.56, 60.71, 109.47, 126.93, 128.54, 129.42, 129.50, 135.21, 142.22, 152.58, 159.07, 159.67, 167.01; HRMS (ESI) m/z: $[M+Na]^+$ calc = 411.0836; found 411.0836 for $C_{18}H_{17}ClN_4O_4$.

*4.2.18. 3,4,5-Trimethoxy-N-(5-(4-methoxyphenyl)–2H-1,2,4-triazol-3-yl)benzamide (**10f**)*

White powder (0.25 g, 65.7% yield), m.p. 206–208 °C, IR (KBr) υ_{max} (cm^{-1}) 3420, 3245 (NH, NH-amide), 1655 (C=O); ^1H NMR (400 MHz, DMSO d_6) δ (ppm): 3.74 (s, 3H, OCH_3), 3.84 (s, 3H, OCH_3), 3.87 (s, 6H, $2OCH_3$), 7.06 (d, 2H, J = 8.8 Hz, Ar-H), 7.28 (s, 2H, Ar-H), 7.92 (d, 2H, J = 8.8 Hz, Ar-H), 10.36 (s, 1H, CO-NH), 10.40 (s, 1H, NH); ^{13}C NMR (100 MHz, DMSO d_6) δ (ppm): 55.86, 56.48, 60.61, 105.42, 114.23, 114.37, 125.10, 128.08, 129.80, 140.85, 153.15, 162.53, 165.89, 166.04; HRMS (ESI) m/z: $[M-H]^-$ calc = 383.1434; found 383.1230 for $C_{19}H_{20}N_4O_5$.

*4.2.19. N-(5-(3-Chlorophenyl)-2H-1,2,4-triazol-3-yl)-3,4,5-trimethoxybenzamide (**10g**)*

White powder (0.26 g, 69% yield), m.p. 186–188 °C, IR (KBr) υ_{max} (cm^{-1}) 3390, 3230 (NH, NH-amide), 1650 (C=O); ^1H NMR (400 MHz, DMSO d_6) δ (ppm): 3.83 (s, 3H, OCH_3), 3.85 (s, 6H, $2OCH_3$), 7.27 (s, 2H, Ar-H),), 7.59 (t, 1H, J = 7.6 Hz, Ar-H), 7.70 (d, 1H, J = 8.0 Hz, Ar-H), 7.90 (d, 1H, J = 7.6 Hz, Ar-H), 7.97 (s, 1H, Ar-H), 10.53 (s, 1H, CO-NH), 10.65 (s, 1H, NH); ^{13}C NMR (100 MHz, DMSO d_6) δ (ppm): 56.49, 60.60, 105.45, 126.66, 127.70, 127.86,

131.14, 132.27, 133.86, 134.96, 140.94, 141.20, 153.17, 156.08, 165.67; HRMS (ESI) *m/z*: $[M+Na]^+$ calc = 411.0836; found 411.0822 for $C_{18}H_{17}ClN_4O_4$.

4.3. General method for synthesis of 5-amino-3-(substituted phenyl)-N-phenyl or ethyl-1H-1,2,4-triazole-1-carbothioamide (**11a-f**)

A mixture of triazole **7b, 7c** or **7d** (1 mmol) and the appropriate ethyl or phenyl isothiocyanate (1 mmol) in ethanol (20 mL) was stirred for 3 h. The formed solid was filtered off, dried and crystallized from ethanol to obtain compounds **11a-f.**

4.3.1. 5-Amino-3-(3,4,5-trimethoxyphenyl)-N-phenyl-1H-1,2,4-triazole-1-carbothioamide (**11a**)

White powder (0.23 g, 62% yield), m.p. 190–191 °C, IR (KBr) υ_{max} (cm^{-1}) 3450, 3410, 3350 (NH, NH-CS, CS-NH); ^1H NMR (400 MHz, DMSO d_6) δ (ppm): 3.72 (s, 3H, OCH_3), 3.84 (s, 6H, $2OCH_3$), 7.16–7.18 (m, 1H, Ar-H), 7.29 (s, 2H, Ar-H), 7.31–7.35 (m, 2H, Ar-H), 7.45 (d, 2H, J = 8.4 Hz, Ar-H), 9.72 (s, 1H, NH), 9.77 (s, 1H, NH), 10.50 (s, 1H, NH); ^{13}C NMR (100 MHz, DMSO d_6) δ (ppm): 56.56, 60.62, 105.96, 125.51, 126.48, 128.13, 128.49, 131.20, 139.75, 140.96, 158.30, 165.30, 181.20; HRFAB-MS *m/z* $[M-H]^-$ calc = 384.1130;found 384.1129 for $C_{18}H_{19}N_5O_3S$.

4.3.2 5-Amino-N-ethyl-3-(3,4,5-trimethoxyphenyl)-1H-1,2,4-triazole-1-carbothioamide (**11b**)

White powder (0.22 g, 65% yield), m.p. 203–205 °C, IR (KBr) υ_{max} (cm^{-1}) 3400, 3330, 3280 (NH, NH-CS, CS-NH); ^1H NMR (400 MHz, DMSO d_6) δ (ppm): 1.07 (t, 3H, J = 6.80 Hz, CH_3), 3.49 (q, 2H, J = 6.8 Hz, CH_2), 3.71 (s, 3H, OCH_3), 3.84 (s, 6H, $2OCH_3$), 7.26 (s, 2H, Ar-H), 8.06 (s, 1H, NH), 9.25 (s, 1H, NH), 10.27 (s, 1H, NH); ^{13}C NMR (100 MHz, DMSO d_6) δ (ppm): 14.94, 40.34, 56.55, 60.62, 105.90, 127.99, 130.26, 140.97, 153.00, 165.77, 181.76; HRFAB-MS *m/z* $[M-H]^-$ calc = 336.1209;found 336.1001 for $C_{14}H_{19}N_5O_3S$.

4.3.3. 5-Amino-3-(4-methoxyphenyl)-N-phenyl-1H-1,2,4-triazole-1-carbothioamide (**11c**)

White powder (0.25 g, 78% yield), m.p. 181–183 °C, IR (KBr) υ_{max} (cm^{-1}) 3450, 3400, 3320 (NH, NH-CS, CS-NH); ^1H NMR (400 MHz, DMSO d_6) δ (ppm): 3.83 (s, 3H, OCH_3), 7.04 (d, 2H, J = 8.8 Hz, Ar-H), 7.13–7.17 (m, 1H, Ar-H), 7.31–7.35 (m, 2H, Ar-H), 7.45 (s, 2H, Ar-H), 7.93 (d, 2H, J = 8.4 Hz, Ar-H), 9.64 (s, 1H, NH), 9.78 (s, 1H, NH), 10.38 (s, 1H, NH); ^{13}C NMR (100 MHz, DMSO d_6) δ (ppm): 55.89, 113.94, 125.18, 125.44, 126.39, 127.60, 128.44, 130.29, 139.74, 162.54, 166.03, 182.20; HRFAB-MS *m/z* $[M-H]^-$ calc = 324.0997; found 324.0778 for $C_{16}H_{15}N_5OS$.

4.3.4. 5-Amino-N-ethyl-3-(4-methoxyphenyl)-1H-1,2,4-triazole-1-carbothioamide (**11d**)

White powder (0.20 g, 73% yield), m.p. 229–231 °C, IR (KBr) υ_{max} (cm^{-1}) 3410, 3370, 3320 (NH, NH-CS, CS-NH); ^1H NMR (400 MHz, DMSO d_6) δ (ppm): 1.07 (t, 3H, J = 8.0 Hz, CH_3), 3.47 (q, 2H, J = 8.0 Hz, CH_2), 3.82 (s, 3H, OCH_3), 7.03 (d, 2H, J = 8.8 Hz, Ar-H), 7.90 (d, 2H, J = 8.8 Hz, Ar-H), 8.06 (s, 1H, NH), 9.18 (s, 1H, NH), 10.17 (s, 1H, NH); ^{13}C NMR (100 MHz, DMSO d_6) δ = 14.96, 38.97, 55.89, 113.94, 125.11, 130.21, 162.53, 166.02, 181.88; HRFAB-MS *m/z* $[M-H]^-$ calc = 276.0997; found 276.0780 for $C_{12}H_{15}N_5OS$.

4.3.5. 5-Amino-3-(3-chlorophenyl)-N-phenyl-1H-1,2,4-triazole-1-carbothioamide (**11e**)

White powder (0.24 g, 73% yield), m.p. 179–181 °C, IR (KBr) υ_{max} (cm^{-1}) 3380, 3340, 3300 (NH, NH-CS, CS-NH); ^1H NMR (400 MHz, DMSO d_6) δ (ppm): 7.13–7.17 (m, 1H, Ar-H), 7.31–7.35 (m, 2H, Ar-H), 7.45 (s, 2H, Ar-H), 7.49–7.57 (m, 1H, Ar-H), 7.67 (d, 1H, J = 8.0 Hz, Ar-H), 7.90 (d, 1H, J = 8.0 Hz, Ar-H), 8.02 (s, 1H, Ar-H), 9.75 (s, 1H, NH), 9.84 (s, 1H, NH), 10.67 (s, 1H, NH); ^{13}C NMR (100 MHz, DMSO d_6) δ (ppm): 125.66, 127.07, 127.26, 128.20, 128.53, 130.79, 131.42, 132.12, 133.54, 135.04, 139.63, 165.24, 181.68; Elemental analysis for $C_{15}H_{12}ClN_5S$ (328.1), Calculated; C, 54.63; H, 3.67; N, 21.23; Found C, 54.80; H, 3.84; N, 21.51.

4.3.6. 5-Amino-3-(3-chlorophenyl)-N-ethyl-1H-1,2,4-triazole-1-carbothioamide (**11f**)

White powder (0.23 g, 83% yield), m.p. 194–195 °C, IR (KBr) υ_{max} (cm^{-1}) 3400, 3350, 3300 (NH, NH-CS, CS-NH); ^1H NMR (400 MHz, DMSO d_6) δ (ppm): 1.07 (t, 3H, J = 6.80 Hz, CH_3), 3.48 (q, 2H, J = 6.80 Hz, CH_2), 7.56 (t, 1H, J = 5.6 Hz, Ar-H), 7.66 (d, 1H, J = 8.0 Hz, Ar-H), 7.86 (d, 1H, J = 8.0 Hz, Ar-H), 7.97 (s, 1H, Ar-H), 8.15 (s, 1H, NH), 9.27 (s, 1H, NH), 10.43 (s, 1H, NH); ^{13}C NMR (100 MHz, DMSO d_6) δ = 14.92, 40.31, 127.01, 128.12, 130.78, 132.09, 133.54, 133.67, 134.99, 162.21, 181.75; Elemental analysis for $C_{11}H_{12}ClN_5S$ (280.1), Calculated; C, 46.89; H, 4.29; N, 24.86; Found C, 47.12; H, 4.38; N, 25.11.

4.4. Biological evaluation

4.4.1. MTT assay

MTT assay was performed to investigate the effect of the synthesized compounds on mammary epithelial cells (MCF-10A) [53]. The cells were propagated in medium consisting of Ham's F-12 medium/Dulbecco's modified Eagle's medium (DMEM) (1:1) supplemented with 10% foetal calf serum, 2 mM glutamine, insulin (10 μg/mL), hydrocortisone (500 ng/mL) and epidermal growth factor (20 ng/mL). Trypsin ethylenediamine tetra acetic acid (EDTA) was used to passage the cells after every 2–3 days. 96-well flat-bottomed cell culture plates were used to seed the cells at a density of 10^4 cells mL^{-1}. The medium was aspirated from all the wells of culture plates after 24 h followed by the addition of synthesized compounds (in 200 μL medium to yield a final concentration of 0.1% (v/v) dimethylsulfoxide) into individual wells of the plates. Four wells were designated to a single compound. The plates were allowed to incubate at 37 °C for 96 h. Afterwards, the medium was aspirated and 3-[4,5-dimethylthiazol-2-yl]-2,5-diphenyltetrazolium bromide (MTT) (0.4 mg/mL) in medium was added to each well and subsequently incubated for 3 h. The medium was aspirated and 150 μL dimethyl sulfoxide (DMSO) was added to each well. The plates were vortexed followed by the measurement of absorbance at 540 nm on a microplate reader. The results were presented as inhibition (%) of proliferation in contrast to controls comprising 0.1% DMSO.

4.4.2. Assay for antiproliferative effect

Propidium iodide fluorescence assay [53] was carried out on Panc-1(pancreas cancer), PaCa-2 (pancreatic carcinoma), MCF-7 (breast cancer): A-549 (epithelial): HT-29 (colon cancer), H-460 (lung cancer) and *PC*-3 (prostate cancer) cell lines to investigate the antiproliferative activity of compounds. Propidium iodide is a fluorescence dye which possesses ability to attach with DNA, therefore providing a precise and quick method for the calculation of total nuclear DNA. PI is incapable of crossing the plasma membrane and its fluorescence signal intensity is directly proportional to the amount of cellular DNA. Thus, cells with damaged plasma membranes or altered permeability are totaled as dead ones. To perform the assay, cells were seeded in 96-well flat-bottomed culture plates at a density of 3000–7500 cells/well in 200 μL medium and incubated at 37 °C for 24 h in humidified 5% CO_2/95% air atmosphere. Later, the compounds at 10 μM concentrations (in 0.1% DMSO) were added in triplicate wells while 0.1% DMSO served as control, followed by a 48 h incubation of plates. The medium was removed and 25 μL PI (50 μg/mL in water/medium) was added in each well. The plates were then frozen at −80 °C for 24 h, followed by thawing and equilibration to 25 °C. The readings were recorded

at excitation and emission wavelengths of 530 and 620 nm using a fluorometer (Polar-Star BMG Tech). Following formula was used to calculate the cytotoxicity (%) of compounds:

$$\%\text{Cytotoxicity} = \frac{A_C - A_{TC}}{A_C} \times 100$$

where A_C = Absorbance of control and A_{TC} = Absorbance of treated cells. To equate the results, erlotinib was used as positive control.

4.4.3. Tubulin polymerization assay

The activity of compounds on tubulin polymerization was investigated by Tubulin Polymerization Assay Kit (Cytoskeleton Inc., Denver, CO, USA), which works via fluorescent reporter enhancement. The fluorescence of compounds (dissolved in DMSO at 5 and 25 μM concentration) was recorded in triplicates using FLUO star OPTIMA. Docetaxel and vincristine (Apoteket AB, Sweden) served as positive stabilizing and destabilizing controls. Both were used at 3 μM concentration in PBS [54].

4.4.4. EGFR inhibitory assay

Baculoviral expression vectors such as pFASTBacHTc and pBlueBacHis2B were separately used to clone 1.6 kb cDNA encoding for EGFR cytoplasmic domain (EGFR-CD, amino acids (645–1186) were cloned into), separately. A sequence that encodes $(His)_6$ was located at the 5′ upstream to the HER-2 and EGFR sequences. For protein expression, Sf-9 cells were infected for 3 days. Sf-9 cell pellets were solubilized at pH 7.4 at 0 °C for 20 min in a buffer comprising 16 μg/mL benzamidine HCl, 10 μg/mL pepstatin, 10 μg/mL leupeptin, 10 μg/mL aprotinin, 100 μM sodium vanadate, 10 μM ammonium molybdate, 1% Triton, 10 mM NaCl and 50 mM HEPES, followed by 20 min centrifugation. Using an equilibrated Ni-NTA superflow packed column, the crude extract supernatant was passed through and washed first with 10 mM and later with 100 mM imidazole for the elimination of nonspecifically bound material. Histidine-tagged proteins were eluted first with 250 and later with 500 mM imidazole followed by dialysis against 10% glycerol, 20 mM HEPES, 50 mM NaCl, and 1 μg/mL each of pepstatin, leupeptin and aprotinin for 2 h. This purification was carried out either on ice or at 4 °C. On the basis of DELFIA/Time-Resolved Fluorometry, EGFR kinase assay was performed to measure the level of autophosphorylation. DMSO (100%) was used to dissolve the compounds, followed by dilution to suitable concentrations using 25 mM HEPES at pH 7.4. In every well, 10 μL (5 ng for EGFR) recombinant enzyme (1:80 dilution in 100 mM HEPES) was incubated with 10 μL compound at 25 °C for 10 min, followed by addition of 10 μL 5× buffer (containing 1 mM DTT, 100 μM Na_3VO_4, 2 mM $MnCl_2$ and 20 mM HEPES) and 20 μL 0.1 mM ATP-50 mM $MgCl_2$ for 1 h. By incubating the enzyme with or without ATP-$MgCl_2$, positive and negative controls were included in every plate. After incubation, liquid was removed, and wash buffer was used to wash the plates thrice. Each well of plate was added with 75 μL (400 ng) europium-labeled antiphosphotyrosine antibody for another 1 h, followed by washing. After adding the enhancement solution, the signal was detected (with excitation and emission at 340 at 615 nm, respectively) using Victor (Wallac Inc.). Following equation was used to calculate the autophosphorylation inhibition (%) by the compounds:

$$100\% - [(\textit{negative control})/(\textit{positive control}) - (\textit{negative control})]$$

The IC_{50} was calculated using the curves of inhibition (%) with eight concentrations of compound. Most of the signal detected by antiphosphotyrosine antibody is from EGFR, as the impurities in the enzyme preparation are quite low.

4.4.5. BRAF kinase assay

Each compound in this study was subjected to V600E mutant BRAF kinase assay in triplicate. 1 μL drug and 4 μL assay dilution buffer were pre-incubated with 7.5 ng mouse full-length GST-tagged $BRAF^{V600E}$ (Invitrogen, PV3849) at 25 °C for 1 h. The assay was started by adding 5 μL solution comprising 200 ng recombinant human full length, *N*-terminal His-tagged MEK1 (Invitrogen), 30 mM $MgCl_2$ and 200 μM ATP in assay dilution buffer, followed by continuation at 25 °C for 25 min. Using 5× protein denaturing buffer (LDS) solution (5 μL), the assay was quenched. Further denaturing of protein was performed by heating at 70 °C for 5 min. Electrophoresis was performed at 200 V by loading 10 μL of each reaction into a 15-well 4–12% precast NuPage gel plate (Invitrogen). Once the electrophoresis was finished, the front (containing additional hot ATP) was cut from the gel and subsequently discarded. A phosphor screen was used to develop the dried gel. A reaction containing no inhibitor was used as positive control whereas a reaction without active enzyme served as negative control. ELISA kits (Invitrogen) were used as per manufacturer's protocol to investigate the effect of compounds on cell based pERK1/2 activity in cancer cells.

4.5. Molecular docking study

Studies were performed by MOE (Molecular Operating Environment) software was used in performing this docking simulation study. The 3D structures of tubulin (PDB code; isa0) [58,59], was downloaded from Protein Data Bank website, prepared and the hydrogen atoms were added. The binding sites were generated as volumes of selected co-crystallized ligand; colchicine. Moreover, the bound water molecules were deleted from the utilized protein before the docking run. The docked compounds were then energetically minimized with CHARMm ForceField using ligand minimization tool. The docking process was done according the default protocol settings.

References

[1] Y. Yang, Y.H. Ahn, D.L. Gibbons, Y. Zang, W. Lin, N. Thilaganathan, C.A. Alvarez, D.C. Moreira, C.J. Creighton, P.A. Gregory, G.J. Goodall, J.M. Kuri, J. Clin. Invest. 121 (2011) 1373–1385.
[2] C.D. Simpson, K. Anyiwe, A.D. Schimmer, Cancer Lett. 272 (2008) 177–185.
[3] E. Pérez-Herrero, A. Fernández-Medarde, Eur. J. Pharm. Biopharm. 93 (2015) 52–79.
[4] T.A. Baudino, Targeted cancer therapy: the next generation of cancer treatment, Curr. Drug Discov. Technol. 12 (2015) 3–20.
[5] S.H. Cant, J.A. Pitcher, Mol. Biol. Cell. 16 (2005) 1–13.
[6] A.L. Risinger, N.F. Dybdal-Hargreaves, S.L. Mooberry, Anticancer Res. 35 (2015) 5845–5850.
[7] D. Bates, A. Eastman, Br. J. Clin. Pharmacol. 83 (2017) 255–268.
[8] P.P. Gan, J.A. McCarroll, S.T. Po'uha, K. Kamath, M.A. Jordan, M. Kavallaris, Mol. Cancer Ther. 9 (2010) 1339–1348.
[9] G.J. Brouhard, L.M. Rice, J. Cell Biol. 207 (2014) 323–334.
[10] X. Ouyang, X. Chen, E.L. Piatnitski, A.S. Kiselyov, H.-Y. He, Y. Mao, V. Pattaropong, Y. Yu, K.H. Kim, J. Kincaid, L. Smith, W.C. Wong, S.P. Lee, D. Milligan, A. Malikzay, J. Fleming, J. Gerlak, D. Deevi, J.F. Doody, H.-H. Chiang, S. N. Patel, Y. Wang, R.L. Rolser, P. Kussie, M. Labellea, M.C. Tuma, Bioorg. Med. Chem. Lett. 15 (2005) 5154–5159.
[11] S. Arora, A.F. Gonzalez, K. Solanki, Int J. Pharm. Sci. Rev. Res. 22 (2013) 168–174.
[12] R. Kaur, G. Kaur, P.K. Gill, R. Soni, J. Bariwal Eur. J. Med. Chem. 87 (2014) 89–124.
[13] V.K. Kamboj, P.K. Verma, A. Dhanda, S. Ranjan, Cent. Nerv. Syst. Agents Med. Chem. 15 (2015) 17–22.
[14] A. Bhatnagar, P.K. Sharma, N. Kumar, Int. J. Pharm. Tech. Res. 3 (2011) 268–282.
[15] T. Karabasanagouda, A.V. Adhikari, N.S. Shetty, Eur. J. Med. Chem. 42 (2007) 521–529.
[16] K. Sztanke, T. Tuzimski, J. Rzymowska, K. Pasternak, M. Kandefer-Szerszeń, Eur. J. Med. Chem. 43 (2008) 404–419.
[17] D. Sarigol, A. Uzgoren-Baran, B.C. Tel, E.I. Somuncuoglu, I. Kazkayasi, K. Ozadali-Sari, O. Unsal-Tan, G. Okay, M. Ertan, B. Tozkoparan, Bioorg. Med. Chem. 23 (2015) 2518–2528.

[18] I. Küçükgüzel, E. Tatar, S.G. Küçükgüzel, S. Rollas, E. De Clercq, Eur. J. Med. Chem. 43 (2008) 381–392.
[19] A. Kamal, S. Bajee, N.V. Lakshma, S.R.A. Venkata, B. Nagaraju, R.C. Ratna, S.K. Jeevak, A. Alarifi, Bioorg. Med. Chem. Lett. 26 (2016) 2957–2964.
[20] V.K. Patel, H. Rajak, Synthesis, Bioorg. Med. Chem. Lett. 26 (2016) 2115–2118.
[21] A.J. Engdahl, E.A. Torres, S.E. Lock, T.B. Engdahl, P.S. Mertz, C.N. Streu, Org. Lett. 17 (2015) 4546–4549.
[22] H.P. Hsieh, J.P. Liou, N. Mahindroo, Curr. Pharm. Des. 11 (2005) 1655–1677.
[23] V. Chaudhary, J.B. Venghateri, H.P. Dhaked, A.S. Bhoyar, S.K. Guchhait, D. Panda, J. Med. Chem. 59 (2016) 3439–3451.
[24] N.R. Madadi, N.R. Penthala, K. Howk, A. Ketkar, R.L. Eoff, M.J. Borrelli, P.A. Crooks, Eur. J. Med. Chem. 103 (2015) 123–132.
[25] Y.J. Qin, Y.J. Li, A.Q. Jiang, M.R. Yang, Q.Z. Zhu, H. Dong, H.L. Zhu, Eur. J. Med. Chem. 94 (2015) 447–457.
[26] U. Galli, C. Travelli, S. Aprile, E. Arrigoni, S. Torretta, G. Grosa, A. Massarotti, G. Sorba, P.L. Canonico, A.A. Genazzani, G.C. Tron, J. Med. Chem. 58 (2015) 1345–1357.
[27] Q. Zhang, Y. Peng, X.I. Wang, S.M. Keenan, S. Arora, W.J. Welsh, J. Med. Chem. 50 (2007) 749–754.
[28] R. Romagnoli, P.G. Baraldi, M.K. Salvador, F. Prencipe, V. Bertolasi, M. Cancellieri, A. Brancale, E. Hamel, I. Castagliuolo, F. Consolaro, E. Porcù, G. Basso, G. Viola, J. Med. Chem. 57 (2014) 6795–6808.
[29] K. Dornberger, V. Bockel, J. Heyer, C.L. Schonfeld, M. Tonew, E. Tonew, L Pharmazie 30 (1975) 1029–1034.
[30] S.J. Kaiser, N.T. Mutters, B. Blessing, F. Günther, Fitoterapia 119 (2017) 57–63.
[31] M. Wos, M. Miazga-Karska, A.A. Kaczor, K. Klimek, Z. Karczmarzyk, D. Kowalczuk, W. Wysocki, G. Ginalska, Z. Urbanczyk-Lipkowska, M. Morawiak, M. Pitucha, Biomed Pharmacother. 93 (2017) 1269–1276.
[32] K. Xu, P.J. Ornalley, Biochem. Pharmacol. 60 (2000) 221–231.
[33] K. Xu, P.G. Ornalley, Br. J. Cancer 84 (2001) 670–673.
[34] C.J. Xu, G.X. Shen, X.L. Yuan, J.H. Kim, A. Gopalkrishnan, Y.S. Keum, S.A.N. Nair, Carcinogenesis 27 (2006) 437–445.
[35] E. Tseng, E.A. Scott-Ramsay, M.E. Morris, Exp. Biol. Med. 229 (2004) 835–842.
[36] Y.F. Kuang, Y.H. Chen, Food Chem. Toxicol. 42 (2004) 1711–1718.
[37] L.X. Mi, X.T. Wang, S. Govind, B.L. Hood, T.D. Veenstra, T.P. Conrads, D.T. Saha, R. Goldman, F.L. Chung, Cancer Res. 67 (2007) 6409–6416.
[38] R. Yu, J.J. Jiao, J.L. Duh, T.H. Tan, A.N.T. Kong, Cancer Res. 56 (1996) 2954–2959.
[39] R. Hu, B.R. Kim, C. Chen, V. Hebbar, A.N.T. Kong, Carcinogenesis 24 (2003) 1361–1367.
[40] R. Yu, S. Mandlekar, K.J. Harvey, D.S. Ucker, A.N.T. Kong, Cancer Res. 58 (1998) 402–408.
[41] K. Xu, P.J. Thornalley, Biochem. Pharmacol. 61 (2001) 165–177.
[42] Y.S. Zhang, L. Tang, V. Gonzalez, Mol. Cancer ther. 2 (2003) 1045–1052.
[43] D. Xiao, S.K. Srivastava, K.L. Lew, Y. Zeng, P. Hershberger, C.S. Johnson, D.L. Trump, S.V. Singh, Carcinogenesis 24 (2003) 891–897.
[44] D. Xiao, S.V. Singh, Cancer Res. 67 (2007) 2239–2246.
[45] R.H. Dashwood, E. Ho, Nutr. Rev. 66 (2008) S36–S38.
[46] T. Hasegawa, H. Nishino, A. Iwashima, Anticancer Drugs 4 (1993) 273–279.
[47] V.M. Chernyshev, E.V. Tarasova, V. Chernysheva, V. Taranushich, Russ. J. Appl. Chem. 84 (2011) 1890–1896.
[48] A.V. Dolzhenko, A.V. Dolzhenko, W.K. Chui, Tetrahedron 63 (2007) 12888–12895.
[49] D. Kadadevar, K.C. Chaluvaraju, M.S. Niranjan, C. Sultanpur, S.K. Madinur, H.M. Nagaraj, M. Smitha, K. Chakraborty, Int. J. Chem. Tech. Res. 3 (2011) 1064–1069.
[50] A.V. Dolzhenko, G. Pastorin, A.V. Dolzhenko, W.K. Chui, Tetrahedron Lett. 50 (2009) 2124–2128.
[51] S. Ahmed, M. Zayed, S. El-Messery, M. Al-Agamy, H. Abdel-Rahman, Molecules 21 (2016) 568–584.
[52] Y. Sato, Y. Shimoji, H. Fujita, H. Nishino, H. Mizuno, S. Kobayashi, S. Kumakura, J. Med. Chem. 23 (1980) 927–937.
[53] H.L. Qin, J. Leng, B.G. Youssif, M.W. Amjad, M.A. Raja, M.A. Hussain, Z. Hussain, S.N. Kazmi, S.N. Bukhari, Chem. Biol. Drug Des. (2017) 1–7.
[54] G.F. Zha, H.L. Qin, B.G. Youssif, M.W. Amjad, M.A. Raja, A.H. Abdelazeem, S.N. Bukhari, Eur. J. Med. Chem. 135 (2017) 34–48.
[55] R. Romagnoli, P.G. Baraldi, M.K. Salvador, F. Prencipe, V. Bertolasi, M. Cancellieri, A. Brancale, E. Hamel, I. Castagliuolo, F. Consolaro, E. Porcù, G. Basso, G. Viola, Synthesis, antimitotic and antivascular activity of 1-(3',4',5'-trimethoxybenzoyl)-3-arylamino-5-amino- 1,2,4-triazoles, J. Med. Chem. 57 (2014) 6795–6808.
[56] B. Miao, I. Skidan, V. Yang, Z. You, X. Fu, M. Famulok, B. Schaffhausen, V. Torchilin, J. Yuan, A. Degterev, Oncogene 31 (2012) 4317–4332.
[57] K. Yadagiri, C. Sinziana, R. Robert, T. Vladimir, D. Alexei, V.R. Chepuri, Med. Chem. Commun. 5 (2014) 1359–1363.
[58] R.B.G. Ravelli, B. Gigant, P.A. Curmi, I. Jourdain, S. Lachkar, A. Sobel, M. Knossow, Nature 428 (2004) 198–202.
[59] Molecular Operating Environment (MOE 2008.10); Chemical Computing Group, Inc., Montreal, Quebec, Canada, 2008; http://www.chemcomp.com.